

**UNCLASSIFIED**



**Australian Government**

**Department of Defence**

Defence Science and  
Technology Group

# Calibration of the Flow in the Test Section of the Research Wind Tunnel at DST Group

*Lincoln P. Erm and Paul P. E. Jacquemin*

**Aerospace Division**

Defence Science and Technology Group

DST Group-TN-1468

## **ABSTRACT**

Results are given of a detailed calibration of the flow in the test section of the Research Wind Tunnel at DST Group. The calibration was performed to establish the flow quality and to provide guidance when determining the suitability of the tunnel for given tests. Longitudinal mean-flow velocities, flow angles and longitudinal-component turbulence intensities were measured at up to 187 grid locations across the flow at the centre of the test section for nominal free-stream velocities of 10 and 20 m·s<sup>-1</sup>. Measurements were taken when screens were installed in the tunnel and when there were no screens in the tunnel. The most important area of the test section, where models are usually located, is the region comprising approximately the central 50% of the cross-sectional area of the test section. In this region, the following flow non-uniformities were observed when screens were in the tunnel. For nominal free-stream velocities of 10 and 20 m·s<sup>-1</sup>, velocity deviations varied by about 0.5%, horizontal and vertical flow angles varied by about 0.6°, and longitudinal-component turbulence intensities were below about 0.3%. The variations in flow parameters are comparable with acceptable variations quoted in the literature. Based on these measurements, the tunnel is considered suitable for flow-visualization studies around models and the measurement of forces, moments and pressures on models. The tunnel may not be suitable for boundary-layer-transition studies, due to the moderate levels of free-stream turbulence levels in the tunnel. Possible ways of modifying the tunnel to improve the flow in the test section are suggested.

**RELEASE LIMITATION**

*Approved for public release*

**UNCLASSIFIED**

UNCLASSIFIED

*Published by*

*Aerospace Division  
DST Group Defence Science and Technology Group  
506 Lorimer St  
Fishermans Bend, Victoria 3207 Australia*

*Telephone: 1300 333 362  
Fax: (03) 9626 7999*

*© Commonwealth of Australia 2015  
AR-016-436  
October 2015*

**APPROVED FOR PUBLIC RELEASE**

UNCLASSIFIED

**UNCLASSIFIED**

# Calibration of the Flow in the Test Section of the Research Wind Tunnel at DST Group

## Executive Summary

The Defence Science and Technology Group (DST Group) has a Research Wind Tunnel that is used for small-scale testing. It is a suction tunnel, with the fan downstream of the test section, and it has an open-return air-flow circuit. The test section has an octagonal cross section which is 800 mm wide and 622.2 mm high. The tunnel has been designed so that screens at the inlet end of the contraction can be easily inserted or removed, but generally the tunnel is used with the screens installed. The maximum velocity obtainable in the test section when the screens are installed is about 28 m·s<sup>-1</sup>.

The flow in the test section of a tunnel is never completely uniform. Detailed measurements need to be taken at a matrix of grid locations across the flow in the empty test section to see how the flow deviates from location to location, i.e. a tunnel needs to be calibrated. Tunnels are calibrated to establish the quality of the flow in the test section.

In this report, results are presented for a comprehensive calibration of the flow in the test section of the tunnel. Longitudinal mean-flow velocities, flow angles and longitudinal-component turbulence intensities were measured in the test section. Data were acquired at 187 grid locations across the flow, at the centre of the test section, for nominal free-stream velocities of 10 and 20 m·s<sup>-1</sup>, with and without screens in the tunnel.

The most important area of the test section, where models are usually located, is approximately the central 70% of the width and 70% of the height, i.e. the central 50% of the cross-sectional area of the test section. In this region, the following flow non-uniformities were observed. For nominal free-stream velocities of 10 and 20 m·s<sup>-1</sup>, when there were screens in the tunnel, velocity deviations varied by about 0.5%, horizontal and vertical flow angles varied by about 0.6°, and longitudinal-component turbulence intensities were less than about 0.3%.

The literature indicates that, for a low-speed wind tunnel, longitudinal velocities should not deviate from the mean value by more than ±0.75%, and horizontal and vertical flow angles should not deviate from the longitudinal direction by more than ±0.25°. Values of u-component turbulence intensities of 0.1% are low enough for most experiments, but intensities as high as 0.5% are acceptable for developmental testing. For the Research Wind Tunnel, with the screens installed, variations in measured flow parameters in the test section are comparable with acceptable variations reported in the literature. The tunnel is suitable for flow-visualization studies around models and the measurement of forces, moments and pressures on models. The tunnel may not be suitable for boundary-layer-transition studies, due to the moderate levels of free-stream turbulence levels in the tunnel. Possible ways of modifying the tunnel to improve the flow in the test section are suggested.

**UNCLASSIFIED**

## Authors

### **Lincoln P. Erm**

Aerospace Division



*Lincoln Erm obtained a Bachelor of Engineering (Mechanical) degree in 1967 and a Master of Engineering Science degree in 1969, both from the University of Melbourne. His Master's degree was concerned with the yielding of aluminium alloy when subjected to both tensile and torsional loading. He joined the Aeronautical Research Laboratories (now called the Defence Science and Technology Group) in 1970 and has worked on a wide range of research projects, including the prediction of the performance of gas-turbine engines under conditions of pulsating flow, parametric studies of ramrocket performance, flow instability in aircraft intakes and problems associated with the landing of a helicopter on the flight deck of a ship. Concurrently with some of the above work, he studied at the University of Melbourne and in 1988 obtained his Doctor of Philosophy degree for work on low-Reynolds-number turbulent boundary layers. Since this time, he has undertaken research investigations in the low-speed wind tunnel and the water tunnel. He has extended the testing capabilities of the water tunnel, including developing a two-component strain-gauge-balance load-measurement system for the tunnel and developing a dynamic-testing capability for the tunnel, enabling aerodynamic derivatives to be measured on models. Recent work has been concerned with studying the flow around submarine models in the low-speed wind tunnel at DST Group.*

---

### **Paul P. E. Jacquemin**

Aerospace Division



*Paul Jacquemin is a Senior Officer (Technical) in the Aerospace Division at DST Group. He received an Associate Diploma of Engineering (National) in Mechanical Engineering from the Western Melbourne Institute of TAFE. Prior to working at DST Group, he designed the Mechanical and Electrical PLC systems for pneumatic conveying systems. He currently works in the Aircraft Performance and Survivability Branch and conducts aerodynamic tests and provides technical support within the wind tunnel facilities. He recently upgraded the Low Speed Wind Tunnel electrical control and model support systems.*

# Contents

1. INTRODUCTION.....	1
2. MEAN-VELOCITY MEASUREMENTS .....	1
2.1 Test Schedule.....	1
2.2 Procedure Used to Measure Reference Free-Stream Velocities .....	2
2.3 Procedure Used to Measure Mean Velocities.....	3
2.4 Effect of Probe Misalignment With Respect to the Flow .....	4
2.5 Analysis of Mean Velocities .....	4
2.6 Uncertainty in Measured Mean Velocities .....	7
2.7 Boundary-Layer Profiles.....	7
3. FLOW-ANGLE MEASUREMENTS.....	10
3.1 Test Schedule.....	10
3.2 Seven-Hole Probe .....	10
3.3 Procedure Used to Measure Flow Angles .....	10
3.4 Analysis of Flow Angles.....	11
3.5 Uncertainty in Measured Flow Angles .....	16
4. TURBULENCE-INTENSITY MEASUREMENTS.....	16
4.1 Test Schedule.....	16
4.2 Procedure Used to Measure Turbulence Intensities .....	16
4.3 Analysis of Turbulence Intensities .....	17
4.4 Uncertainty in Measured Turbulence Intensities.....	17
5. ASSESSMENT OF FLOW QUALITY IN THE RWT .....	17
5.1 Mean Velocities.....	17
5.2 Flow Angles .....	20
5.3 Turbulence Intensities .....	20
5.4 Adequacy of Flow Quality in the RWT .....	20
6. POSSIBLE WAYS OF IMPROVING THE FLOW IN THE RWT.....	21
7. CONCLUDING REMARKS .....	22
8. ACKNOWLEDGEMENTS .....	23
9. REFERENCES .....	24

## Notation

$C$	Constant used in logarithmic law, $C = 5.2$ .
$H$	Height of test section of Research Wind Tunnel, $H = 622.2$ mm.
$U, V, W$	Instantaneous velocities in the $x_T$ , $y_T$ and $z_T$ directions respectively, ( $\text{m}\cdot\text{s}^{-1}$ ). $U = \bar{U} + u, V = \bar{V} + v, W = \bar{W} + w$ .
$\bar{U}, \bar{V}, \bar{W}$	Mean velocities in the $x_T$ , $y_T$ and $z_T$ directions respectively, ( $\text{m}\cdot\text{s}^{-1}$ ).
$\bar{U}_0$	Velocity at $x_T = 0$ mm, $y_T = 0$ mm and $z_T = 0$ mm, ( $\text{m}\cdot\text{s}^{-1}$ ).
$\bar{U}_{\text{NOM}}$	Nominal free-stream velocity in the $x_T$ direction, ( $\text{m}\cdot\text{s}^{-1}$ ).
$\bar{U}_{\text{REF}}$	Reference free-stream velocity at the “centre” of the test section, ( $\text{m}\cdot\text{s}^{-1}$ ).
$U_\tau$	Friction velocity, $U_\tau = \sqrt{\tau_w/\rho}$ , ( $\text{m}\cdot\text{s}^{-1}$ ).
$u, v, w$	Instantaneous velocity fluctuations from the mean value in the $x_T$ , $y_T$ and $z_T$ directions respectively, ( $\text{m}\cdot\text{s}^{-1}$ ).
$\sqrt{\overline{u^2}}/\bar{U}$	$u$ -component turbulence intensity.
$W$	Width of test section of Research Wind Tunnel, $W = 800.0$ mm.
$x_T, y_T, z_T$	Tunnel coordinate system (right-handed). The $x_T$ axis is horizontal and positive in the downstream direction, the $y_T$ axis is horizontal and is positive to port, and the $z_T$ axis is positive vertically downwards (see Figure 2).
$z$	Distance from floor of test section of Research Wind Tunnel, (m)

### Greek Letters

$\Delta p$	Differential pressure, (Pa)
$\delta_{99}$	Boundary layer thickness corresponding to the location where the velocity in a boundary layer reaches 99% of its free-stream value, (mm).
$\kappa$	Constant used in logarithmic law, $\kappa = 0.41$ .
$\nu$	Kinematic viscosity of air, ( $\text{m}^2\cdot\text{s}^{-1}$ ).
$\rho$	Density of air in test section of RWT, ( $\text{kg}\cdot\text{m}^{-3}$ ).
$\tau_w$	Wall shear stress, (Pa).

### Overlines

– Overlines denote mean values of quantities.

### Acronyms

DST Group	Defence Science and Technology Group.
LSWT	Low-Speed Wind Tunnel.
RWT	Research Wind Tunnel.

# 1. Introduction

The Research Wind Tunnel (RWT) at the Defence Science and Technology Group (DST Group) is used for conducting aerodynamic investigations. The tunnel, shown in Figure 1, has a test section with an octagonal cross section 800 mm wide and 622.2 mm high, and the length of the test section is 1196 mm. The tunnel has been designed so that screens, which are located at the inlet end of the contraction, can be easily installed or removed, but generally the tunnel is used with the screens installed. The cross-sectional shape of the test section of the RWT is geometrically similar to that for the low-speed wind tunnel (LSWT) at DST Group, but the RWT is 3.429 times smaller (linear dimension) than the LSWT. The contraction ratio of both tunnels is 4:1. The maximum velocity obtainable in the test section of the RWT when there are screens in the tunnel is about 28 m·s<sup>-1</sup>. The tunnel has an open return circuit, so that the flow at the outlet of the tunnel returns to the inlet via the laboratory. It is a suction tunnel, with the fan downstream of the test section. Such an arrangement reduces the turbulence intensity in the test section, since turbulent wakes from the fan do not enter the test section.

Ideally, the flow in the test section of a wind tunnel is uniform throughout, is parallel to the test-section walls and has zero turbulence. However, the flow quality is never perfect and it is therefore necessary to calibrate the flow in a tunnel to quantify the extent of the irregularities in the flow. To do this, detailed flow measurements are taken throughout an empty test section to see how the flow varies from location to location. A calibration enables an assessment to be made of the suitability of a tunnel for given tests.

The flow in the test section of the tunnel has recently been calibrated and details of the calibration are given in this report. Mean-flow velocities, flow angles and turbulence intensities were measured at 187 grid locations across the flow at the centre of the test section for nominal free-stream velocities of 10 and 20 m·s<sup>-1</sup>. Calibration data were acquired both with and without the screens in the tunnel. The calibration data are presented and analysed and explanations of flow behaviour are given.

## 2. Mean-Velocity Measurements

### 2.1 Test Schedule

Longitudinal mean velocities,  $\bar{U}$ , were measured in the test section of the tunnel at the 187 grid locations shown in Figure 2 for  $x_T = 0.0$  mm (see below) for nominal free-stream velocities,  $\bar{U}_{\text{NOM}}$ , of 10 and 20 m·s<sup>-1</sup>. Measurements were taken both with and without the screens in the tunnel.

The origin of the tunnel coordinate system,  $x_T$ ,  $y_T$ ,  $z_T$ , shown in Figure 2, is located on the test section longitudinal centreline, half way along the test section. The  $x_T$  axis is positive in the downstream direction, the  $y_T$  axis is horizontal and is positive to the port side of the tunnel, and the  $z_T$  axis is positive vertically downwards. The axes form a right-handed coordinate system and remain fixed with respect to the tunnel.

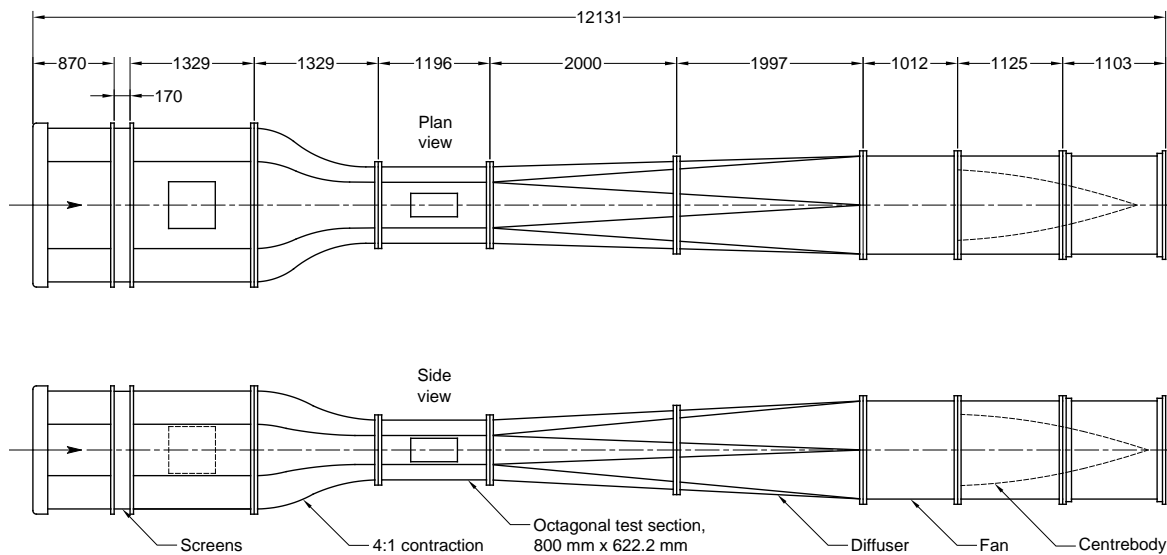


Figure 1 Diagrammatic representation of the RWT.

In Figure 2, the grid points are spaced at intervals of 40.0 mm in the  $y_T$  direction and at intervals of 31.1 mm in the  $z_T$  direction. The  $y_T$  spacing corresponds to 1/20th of the width of the octagonal test section and the  $z_T$  spacing corresponds to 1/20th of the height of the test section ( $W = 800.0$  mm and  $H = 622.2$  mm). The measurement grid for the RWT is geometrically similar to that used by Erm (2003) when calibrating the flow in the test section of the LSWT. For the LSWT, the grid spacing was found to be adequate in terms of establishing spatial variations in flow quantities across the test section.

## 2.2 Procedure Used to Measure Reference Free-Stream Velocities

Reference free-stream velocities,  $\bar{U}_{REF}$ , in the test section of the tunnel were measured using a commercial 90° Pitot-static probe, manufactured by United Sensor<sup>1,2</sup>, mounted on the port wall of the test section and positioned in the free-stream with the tip of the probe located at  $x_T = 400$  mm,  $y_T = 285$  mm and  $z_T = 0$  mm. The total and static pressures from the probe were connected to ports on a Baratron® differential electronic manometer, having a full-scale range of 100 Torr, which corresponds to 100 mm of mercury or about 13330 Pa. The Baratron® was interfaced with a Microstar data-acquisition unit, which was in turn interfaced with a computer, enabling fluctuating differential pressures from the Pitot-static probe to be sampled. The number of samples taken was 15000 and the sampling frequency was 1000 Hz. Free-stream velocities were computed in the conventional manner (see, for example, Rae & Pope, 1984) using  $\bar{U} = \sqrt{2\Delta p/\rho}$ , where  $\Delta p$  is the differential pressure measured by the manometer and  $\rho$  is the density of air. The above sampling parameters resulted in convergence of calculated velocities. Using a larger number of samples or a different sampling rate would not have significantly affected measured velocities.

<sup>1</sup> In this report, the use of trade names for products is for descriptive purposes only and is not an endorsement of the products by DST Group.

<sup>2</sup> Model specification of probe is PAC-12-KL, BSP 1142.

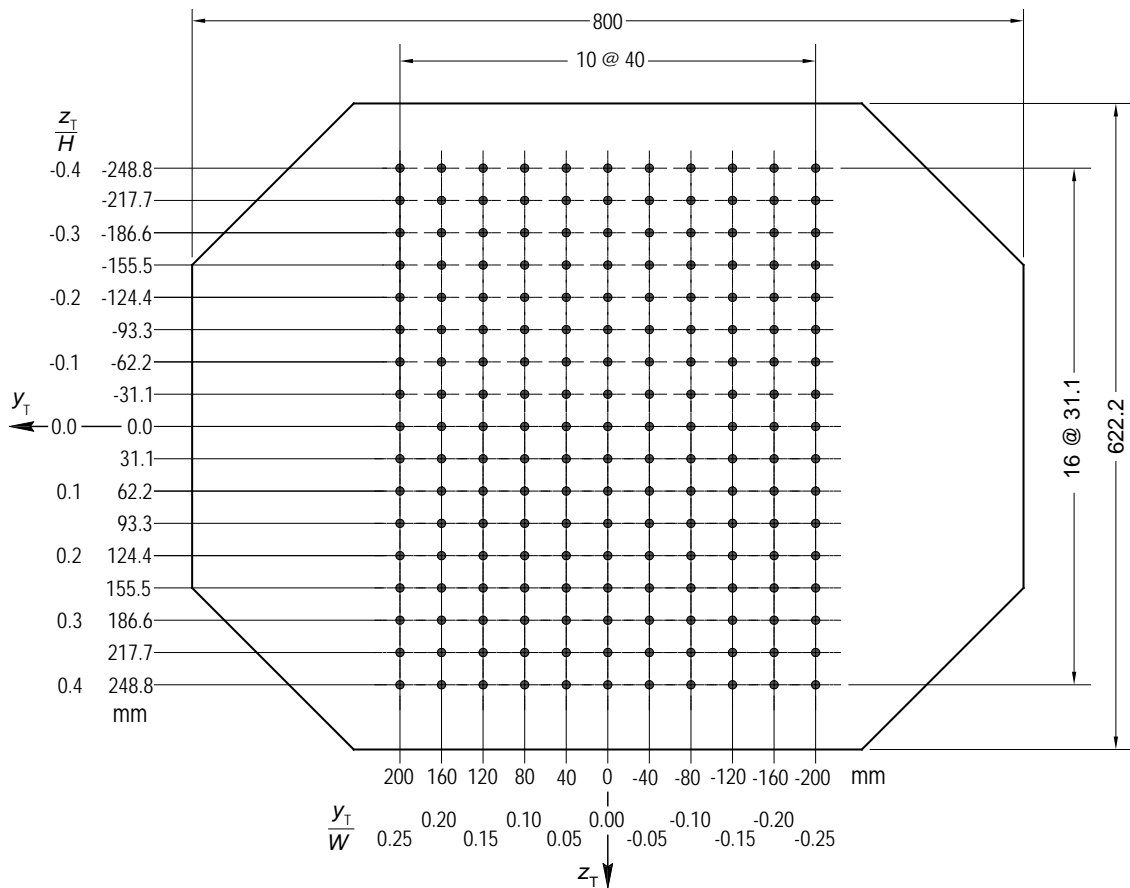


Figure 2 Cross-sectional view of test section of RWT, showing grid locations at which flow measurements were taken. The flow and the positive  $x_T$  axis are out of the page.

### 2.3 Procedure Used to Measure Mean Velocities

Longitudinal mean velocities,  $\bar{U}$ , at the different grid locations in the test section of the RWT were measured using a commercial straight Pitot-static probe, manufactured by United Sensor<sup>3</sup>, which was attached to an overhead traversing mechanism. The probe is shown in Figure 3. The total and static pressures from the probe were connected to ports on a second Baratron<sup>®</sup> differential electronic manometer, having the same full-scale range as that described above for measurement of reference velocities (see Section 2.2). The tip of the probe was manually positioned at the measurement grid, i.e. at  $x_T = 0$  mm, at each  $y_T$  location in turn, and was moved vertically in the  $z_T$  direction using the traversing mechanism. Probe  $x_T$  and  $y_T$  locations could be set to within  $\pm 0.5$  mm and probe  $z_T$  locations could be set to within  $\pm 0.1$  mm. Mean velocities across the grid were determined in a similar manner to that described for reference velocities, (see Section 2.2).

The seven-hole probe used to measure velocities and flow angles (see Section 3) could have been used to measure mean velocities at the different grid locations, but the probe had not been calibrated below Mach 0.2, corresponding to a velocity of about  $68 \text{ m}\cdot\text{s}^{-1}$  (see

<sup>3</sup> Model specification of probe is PBA-8-F-6-KL, Straight, No MC 1148.

Section 3.5). Using this calibration at nominal velocities of 10 and 20 m·s<sup>-1</sup> would have resulted in errors in measured velocities greater than 1%. According to Rae & Pope (1984), a standard Pitot-static probe can be used to measure velocities to an accuracy of about 0.3%, indicating that such a probe is the preferred option to measure velocities in the current investigation compared with the seven-hole probe.

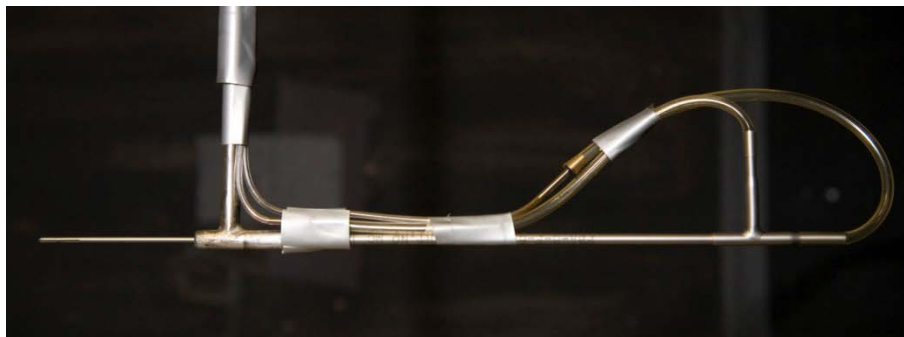


Figure 3 Pitot-static probe set up for measurements in the RWT.

## 2.4 Effect of Probe Misalignment With Respect to the Flow

The likelihood that the flow in the tunnel may be at a slight angle to the longitudinal axis of the Pitot-static probe used for measurements will not affect the test results significantly. Chue (1975) indicates that, for a Pitot-static probe similar to that used in the current investigation, errors in measured total pressures and static pressures due to misalignment of the probe with the flow are negligible for flows whose angle of incidence is within  $\pm 5^\circ$  of the longitudinal axis of a total-pressure probe and within  $\pm 1^\circ$  of the longitudinal axis of a static-pressure probe. The angularity of the flow in the test section is generally less than  $1^\circ$  (see Section 3.4), so that errors in measured pressures and hence velocities will be small.

## 2.5 Analysis of Mean Velocities

When values of  $\bar{U}$  were measured with the Pitot-static probe at the different grid locations, the reference free-stream velocity in the test section,  $\bar{U}_{\text{REF}}$ , generally varied slightly, due to unavoidable drifting of the velocity that often occurred during testing. Consequently, measured values of  $\bar{U}$  at the different grid locations correspond to slightly different values of  $\bar{U}_{\text{REF}}$ . Values of  $\bar{U}$  have therefore been expressed non-dimensionally as velocity deviations  $(\bar{U} - \bar{U}_0)/\bar{U}_0$ , where  $\bar{U}_0$  is the velocity at  $x_T = 0$  mm,  $y_T = 0$  mm and  $z_T = 0$  mm, corresponding to the  $\bar{U}$  measurements at each of the grid locations.

Contours of velocity deviations,  $(\bar{U} - \bar{U}_0)/\bar{U}_0$ , expressed as a percentage, for  $\bar{U}_{\text{NOM}} = 10$  and 20 m·s<sup>-1</sup>, when the screens were in the tunnel, are given in Figure 4. Corresponding plots when the screens were not in the tunnel are given in Figure 5. These contour plots, as well as contour plots of flow angles and turbulence intensities (see Sections 3 and 4 respectively), are presented with the direction of the flow out of the page.

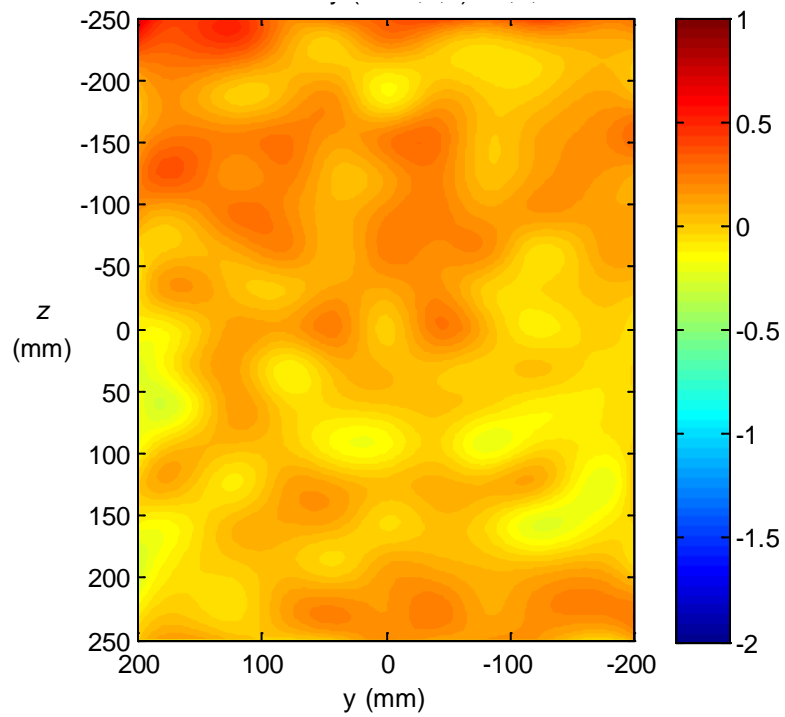
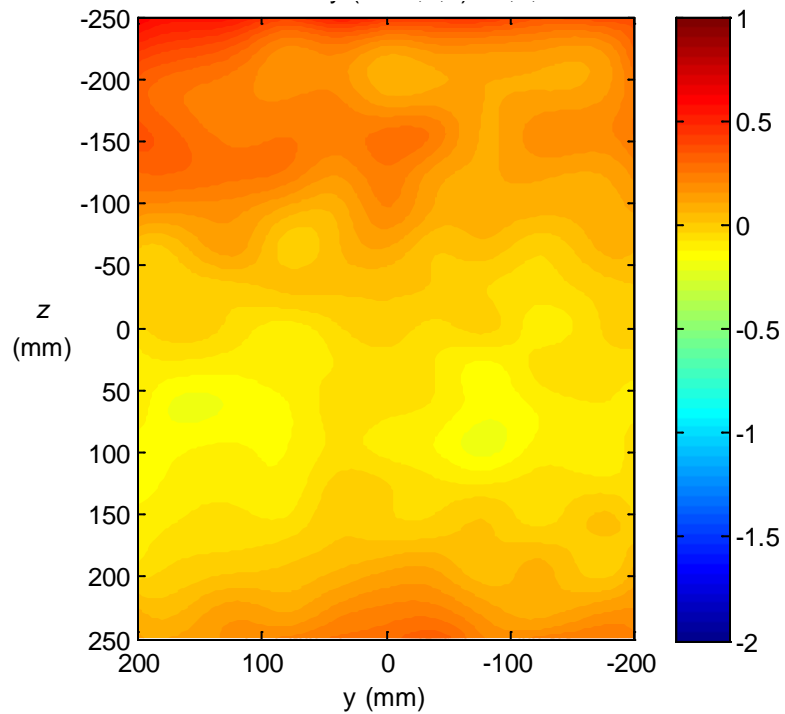
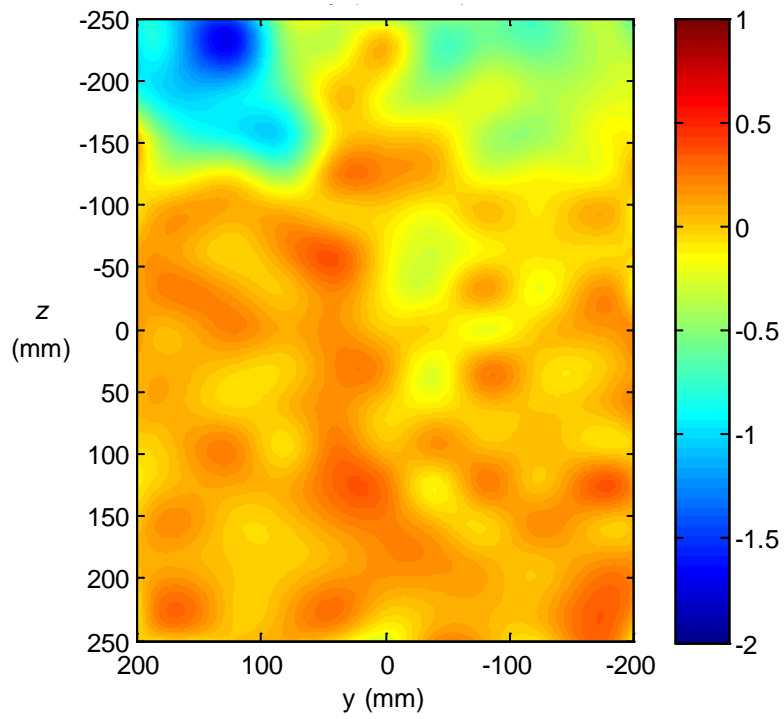
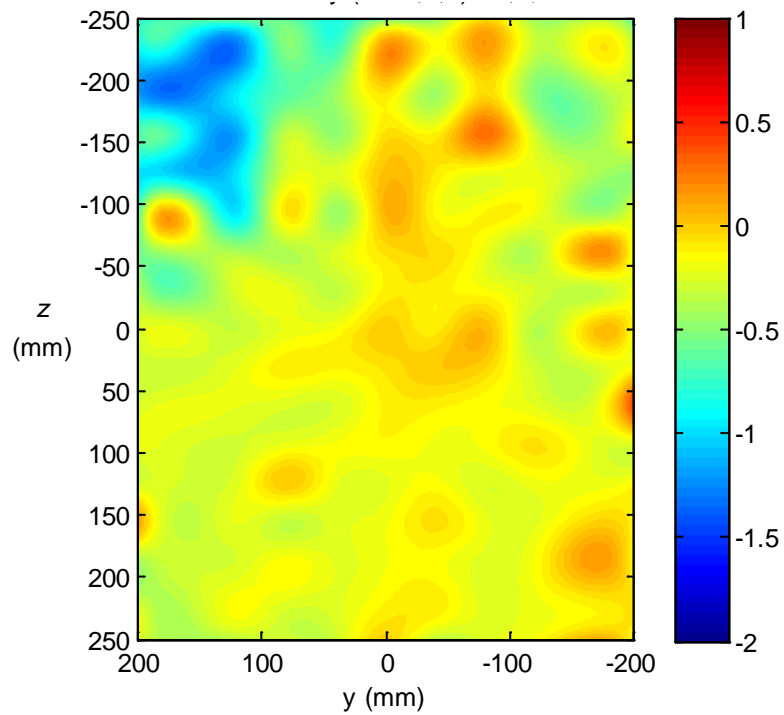
(a)  $\bar{U}_{\text{NOM}} = 10 \text{ m}\cdot\text{s}^{-1}$ .(b)  $\bar{U}_{\text{NOM}} = 20 \text{ m}\cdot\text{s}^{-1}$ .

Figure 4 Contours of velocity deviations,  $(\bar{U} - \bar{U}_0)/\bar{U}_0$  %,  $\bar{U}_{\text{NOM}} = 10$  and  $20 \text{ m}\cdot\text{s}^{-1}$ , screens in tunnel.



(a)  $\bar{U}_{\text{NOM}} = 10 \text{ m}\cdot\text{s}^{-1}$ .



(b)  $\bar{U}_{\text{NOM}} = 20 \text{ m}\cdot\text{s}^{-1}$ .

Figure 5 Contours of velocity deviations,  $(\bar{U} - \bar{U}_0)/\bar{U}_0$  %,  $\bar{U}_{\text{NOM}} = 10$  and  $20 \text{ m}\cdot\text{s}^{-1}$ , screens not in tunnel.

An analysis of Figure 4 shows that the velocity deviations,  $(\bar{U} - \bar{U}_0)/\bar{U}_0$ , vary by about 1% across the grid for  $\bar{U}_{\text{NOM}} = 10$  and  $20 \text{ m}\cdot\text{s}^{-1}$ . Similarly, an analysis of Figure 5 shows that the velocity deviations vary by about 2% across the grid for  $\bar{U}_{\text{NOM}} = 10$  and  $20 \text{ m}\cdot\text{s}^{-1}$ . The variations in velocity deviations are more pronounced near the edges of the grid, particularly at the top of the grid. The greater variation in velocity deviations when the screens were not in the tunnel is to be expected.

## 2.6 Uncertainty in Measured Mean Velocities

There are small uncertainties in measured velocity deviations,  $(\bar{U} - \bar{U}_0)/\bar{U}_0$ , due to small errors in instrumentation readings. It was necessary to measure air temperatures and differential air pressures when calculating mean velocities. Any errors in measured temperatures did not affect velocity deviations as they are expressed as non-dimensional velocity ratios. The indicated readings of the Baratron® differential electronic manometers, used to measure differential pressures, were accurate to within 0.15% of their reading. Uncertainties in velocity deviations are about  $\pm 0.2$  percentage points.

## 2.7 Boundary-Layer Profiles

Boundary layers on the floor of the test section of the RWT were traversed with a Pitot probe at  $x_T = 0 \text{ mm}$  to measure total pressures for  $\bar{U}_{\text{NOM}} = 10$  and  $20 \text{ m}\cdot\text{s}^{-1}$  with the screens in the tunnel. The external diameter of the Pitot probe was  $0.7 \text{ mm}$ . The static pressure in the boundary layers for both cases was assumed to be constant across the layer, and the same as that measured in the tunnel free-stream at  $x_T = 0 \text{ mm}$ . The number of pressures sampled was 15000 and the sampling frequency was 1000 Hz. Using the measured values of total and static pressures, velocities in the boundary layers were determined in a manner similar to that described above for reference velocities, (see Section 2.2).

Plots of  $\bar{U}/U_\tau$  versus  $zU_\tau/\nu$  and  $z$  versus  $\bar{U}$  are shown in Figure 6 for  $\bar{U}_{\text{NOM}} = 10 \text{ m}\cdot\text{s}^{-1}$  and in Figure 7 for  $\bar{U}_{\text{NOM}} = 20 \text{ m}\cdot\text{s}^{-1}$ . The log-law line in Figures 6a and 7a is given by

$$\frac{\bar{U}}{U_\tau} = \left(\frac{1}{\kappa}\right) \ln\left(\frac{zU_\tau}{\nu}\right) + C \quad (1)$$

where  $\kappa = 0.41$ ,  $C = 5.2$  and  $U_\tau = \sqrt{\tau_w/\rho}$  is the friction velocity. It is apparent from Figure 6a, corresponding to  $\bar{U}_{\text{NOM}} = 10 \text{ m}\cdot\text{s}^{-1}$ , that the flow over the floor of the test section is either laminar or transitional, since there is no collapse of data onto the log-law line in the wall region, as occurs for turbulent flow. Figure 7a, corresponding to  $\bar{U}_{\text{NOM}} = 20 \text{ m}\cdot\text{s}^{-1}$ , shows that the flow over the floor of the test section is turbulent, due to collapse of data onto the log-law line.

It can be seen from Figure 6b that the thickness of the boundary layer,  $\delta_{99}$ , is about  $9.5 \text{ mm}$  for  $\bar{U}_{\text{NOM}} = 10 \text{ m}\cdot\text{s}^{-1}$  and from Figure 7b that the thickness is about  $16.5 \text{ mm}$  for  $\bar{U}_{\text{NOM}} = 20 \text{ m}\cdot\text{s}^{-1}$ . It is reasonable to infer that the boundary layers on the walls of the test section do not protrude excessively into the central region of the test section, where models are tested.

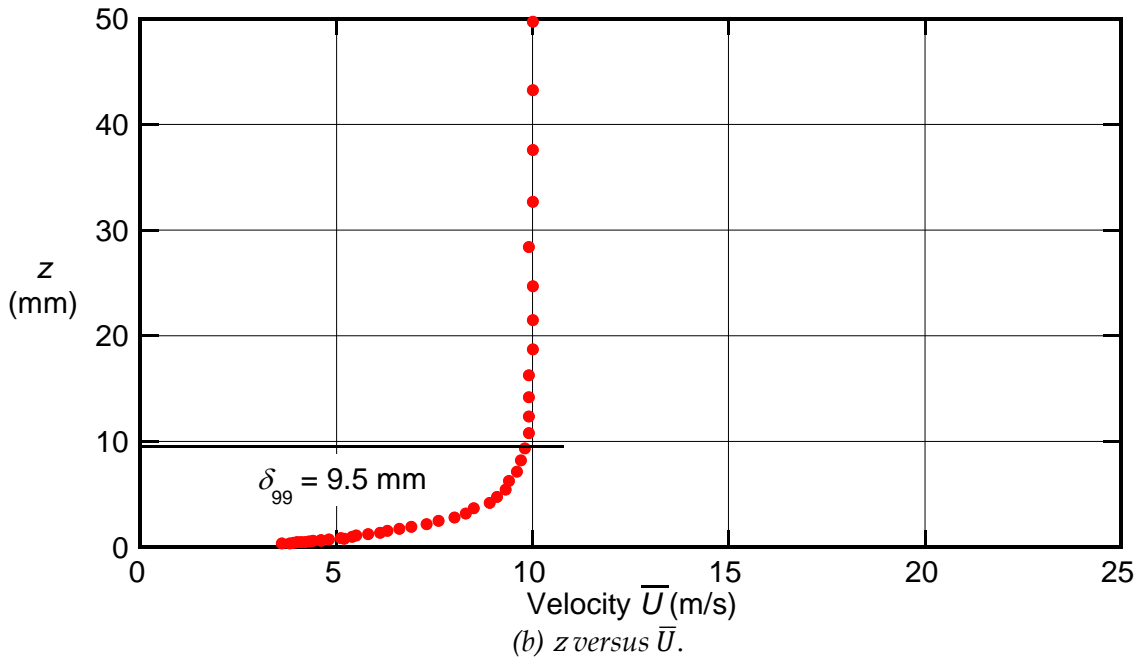
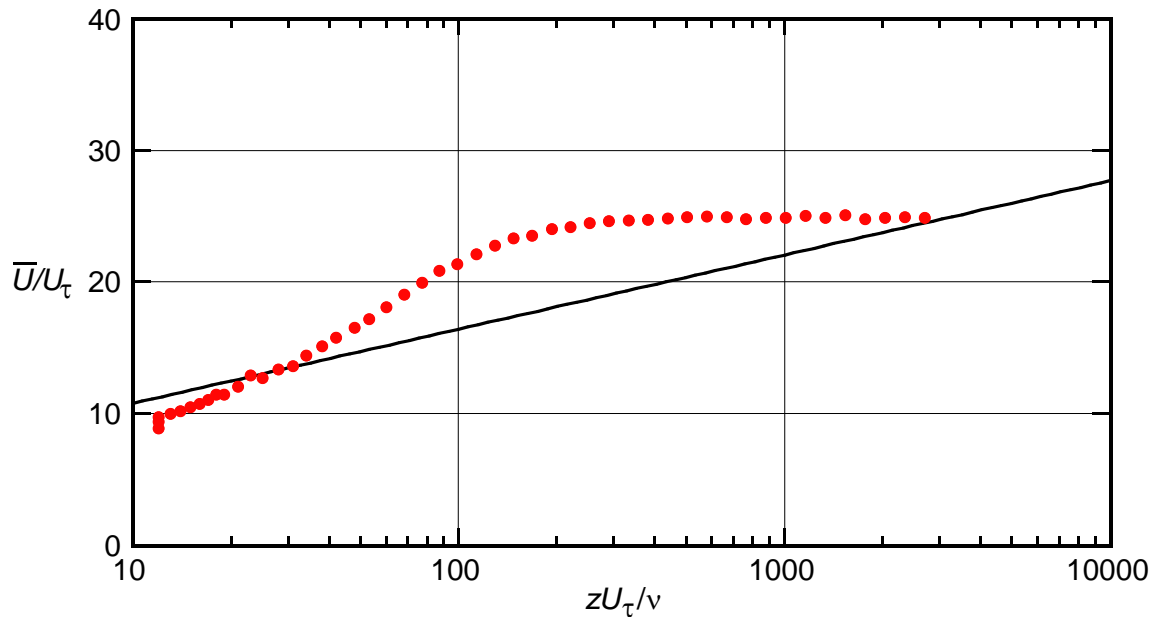


Figure 6 Mean-velocity profiles on the floor of the test section of the RWT,  $\bar{U}_{\text{NOM}} = 10 \text{ m} \cdot \text{s}^{-1}$ , screens in tunnel.

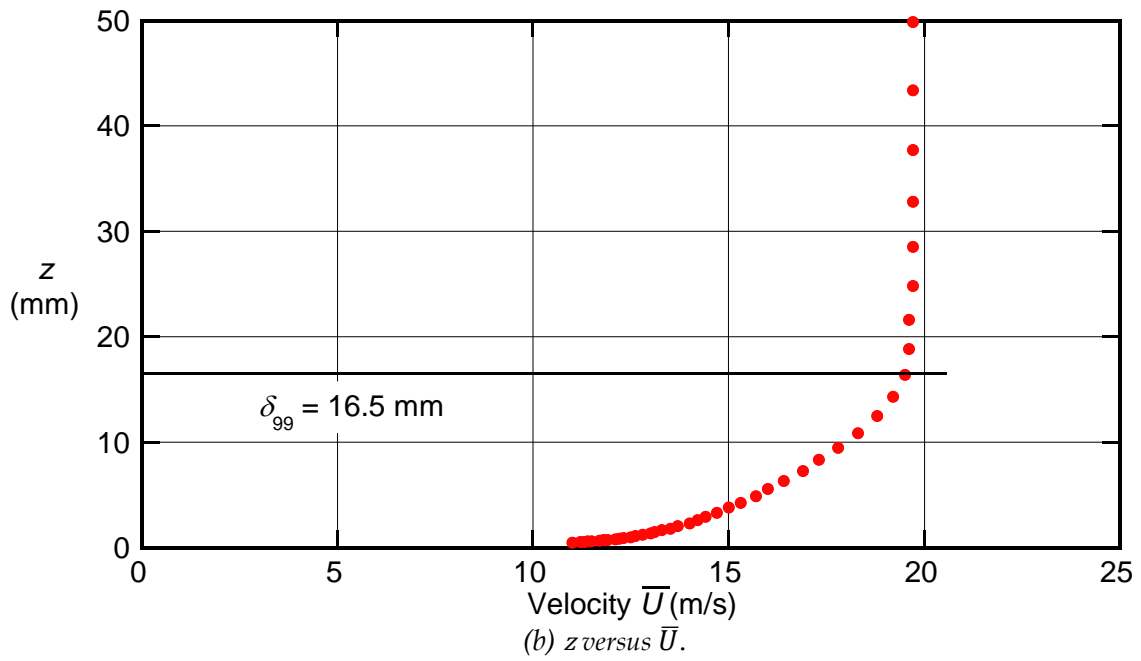
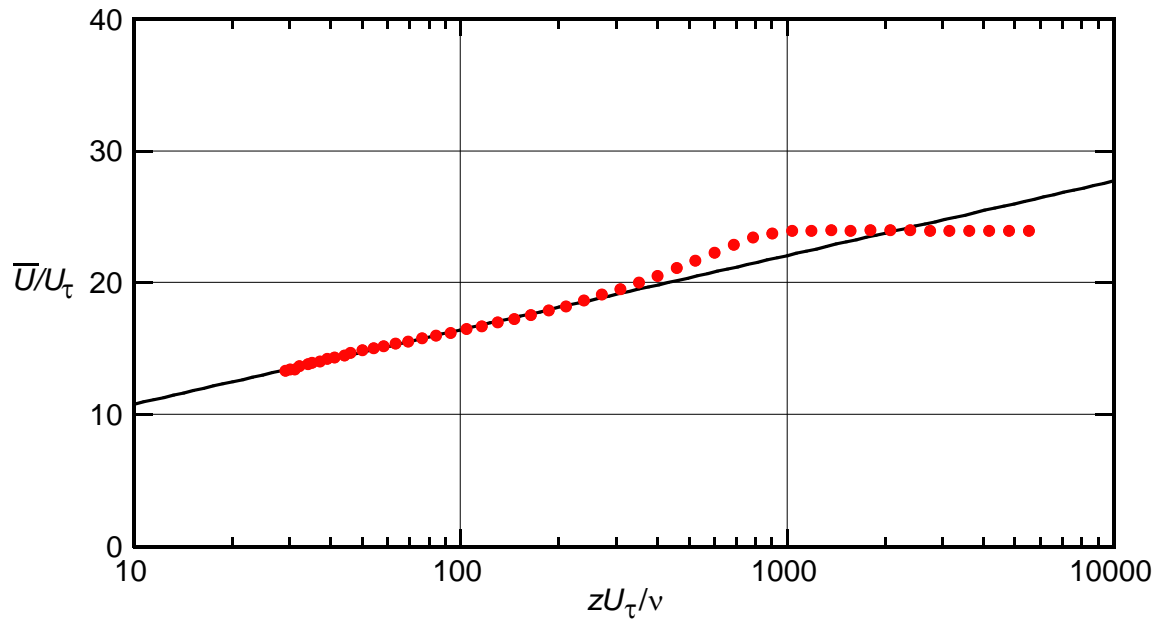


Figure 7 Mean-velocity profiles on the floor of the test section of the RWT,  $\bar{U}_{\text{NOM}} = 20 \text{ m}\cdot\text{s}^{-1}$ , screens in tunnel.

## 3. Flow-Angle Measurements

### 3.1 Test Schedule

Flow angles were measured in the test section of the tunnel at the 187 grid locations shown in Figure 2 at  $x_T = 0.0$  mm for  $\bar{U}_{\text{NOM}} = 10$  and  $20$  m·s<sup>-1</sup>. Measurements were taken both with and without screens in the tunnel.

### 3.2 Seven-Hole Probe

A straight 7-hole probe, manufactured by Aeroprobe Corporation, was used to measure flow angles. The probe is shown mounted in the RWT in Figure 8. The probe has a hemispherical head of diameter 1.66 mm and contains 7 circular pressure tappings. Each of the 7 tappings is connected internally to ports at the downstream end of the probe to enable the individual pressures to be measured. The arrangement of the ports on the head of the probe is shown diagrammatically in Figure 9. A hexagonal mount along the length of the probe is used to attach the probe to a traversing mechanism. The flat faces on the hexagonal mount are stamped with reference marks to ensure that the probe is oriented correctly when measuring flow angles. The probe may contain slight irregularities in the location of the pressure ports, and it is important that the probe is set up as shown. However, any irregularities in the position of the ports do not give erroneous measurements, since the irregularities are accounted for in a probe calibration, provided the probe is set up as shown in Figure 9.

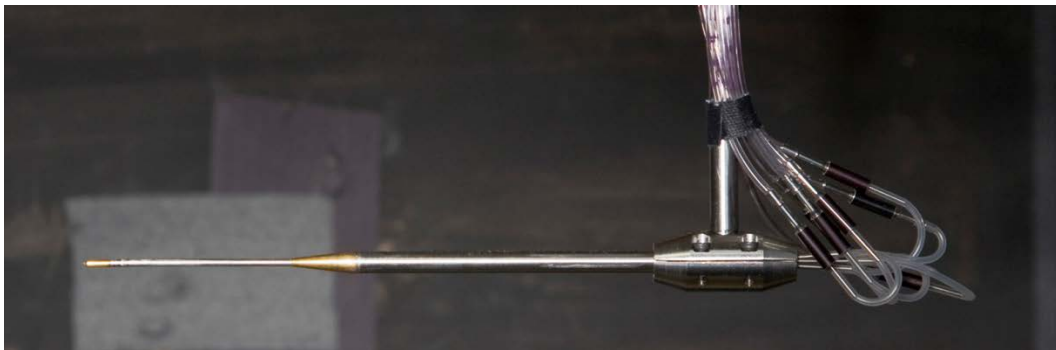


Figure 8 Seven-hole probe set up for measurements in the RWT.

### 3.3 Procedure Used to Measure Flow Angles

Leads from each of the pressure tappings on the 7-hole probe, as well as leads from a reference Pitot-static probe, were connected to ports on a Scanivalve differential electronic manometer, having a full-scale range of 10 inches of water, which corresponds to about 2490 Pa. The Scanivalve was interfaced with a Microstar data-acquisition unit, which was in turn interfaced with the computer, enabling fluctuating pressures from each of the 7 pressure tappings and the reference Pitot-static probe to be sampled. The tip of the probe was manually positioned at the measurement grid, i.e. at  $x_T = 0$  mm, at each  $y_T$  location in

turn, and was moved vertically in the  $z_T$  direction using the traversing mechanism. The pressures at the 7 pressure tapings were each sampled 5000 times at a sampling frequency of 250 Hz. The sampled pressures were processed using Multiprobe software (EXE Version 3.3.1.254, DLL Version 3.3.0.139) to produce mean velocities in the  $x_T$ ,  $y_T$ , and  $z_T$  directions, enabling flow angles in vertical and horizontal planes to be calculated. The above sampling parameters resulted in convergence of calculated mean velocities and flow angles. Flow angles are measured from the positive  $x$  axis. Horizontal flow angles are positive when the flow is towards the port side of the test section and vertical flow angles are positive when the flow is towards the floor of the test section.

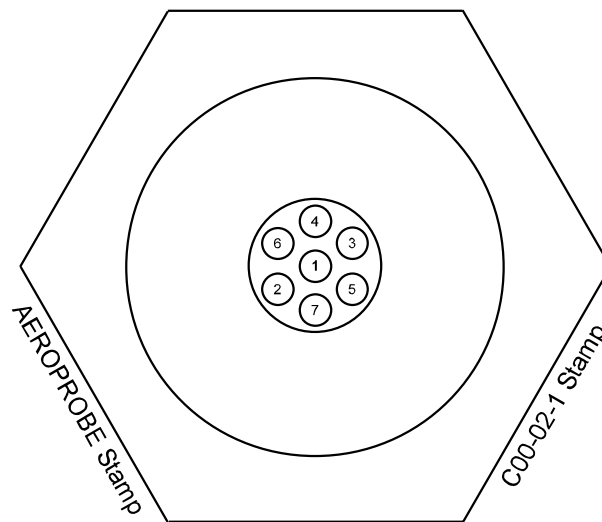


Figure 9 Diagrammatic representation of the layout of the pressure tapings in the hemispherical head of the 7-hole probe, together with the probe hexagonal mount, as viewed looking downstream into the nose of the probe. Diagram is not to scale.

### 3.4 Analysis of Flow Angles

Contours of vertical and horizontal flow angles for  $\bar{U}_{\text{NOM}} = 10$  and  $20 \text{ m}\cdot\text{s}^{-1}$ , when the screens were in the tunnel, are given in Figures 10 and 11 respectively. Similarly, contours of vertical and horizontal flow angles for  $\bar{U}_{\text{NOM}} = 10$  and  $20 \text{ m}\cdot\text{s}^{-1}$ , when the screens were not in the tunnel, are given in Figures 12 and 13 respectively.

Figures 10 and 11, which show contours of vertical and horizontal flow angles for  $\bar{U}_{\text{NOM}} = 10$  and  $20 \text{ m}\cdot\text{s}^{-1}$ , indicate that the range of variation of flow angles is less than  $1^\circ$ . Similarly, Figures 12 and 13, which show contours of vertical and horizontal flow angles for  $\bar{U}_{\text{NOM}} = 10$  and  $20 \text{ m}\cdot\text{s}^{-1}$ , indicate that the range of variation of flow angles is less than  $2^\circ$ . The variations in flow angles are more pronounced near the edges of the grid, particularly at the top of the grid. The greater variation in flow angles with the screens not in the tunnel is as expected.

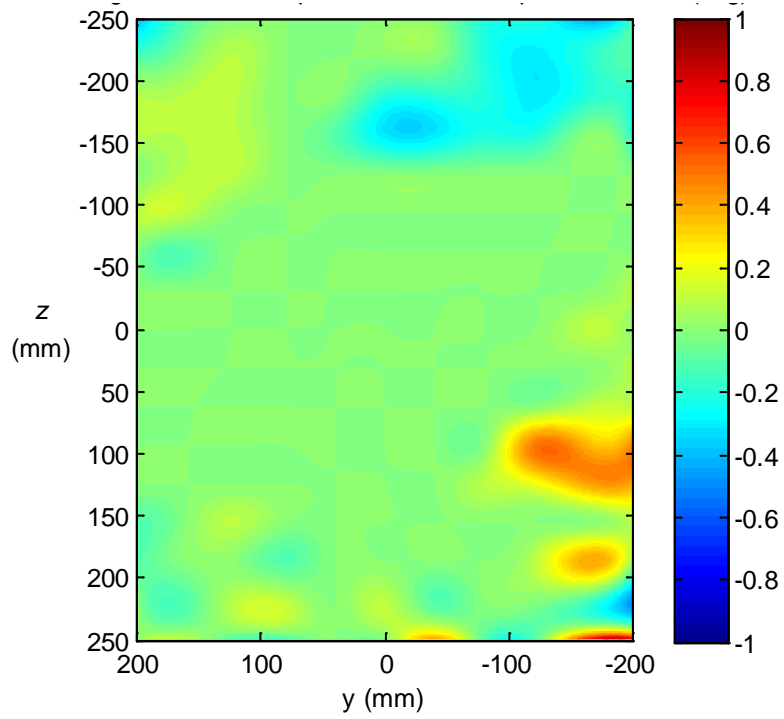
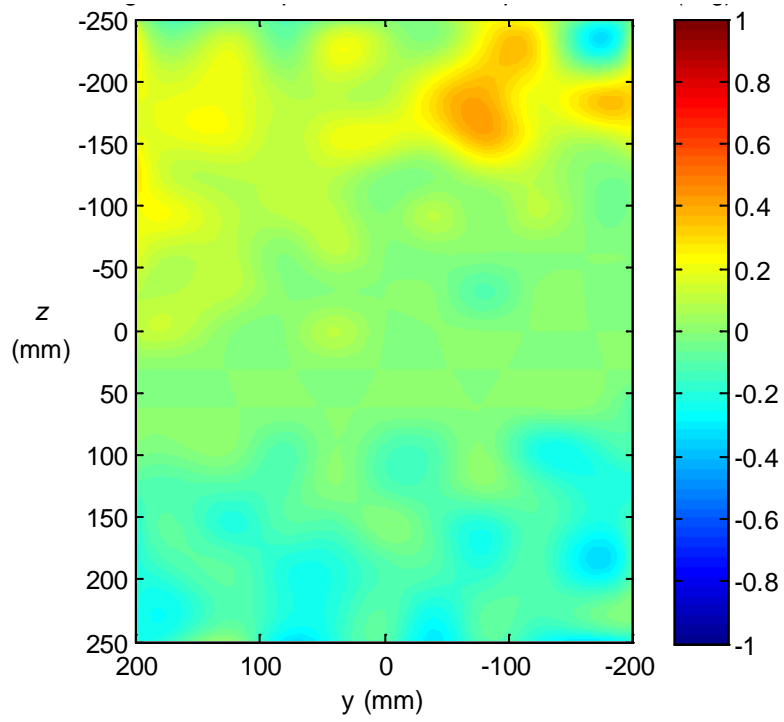
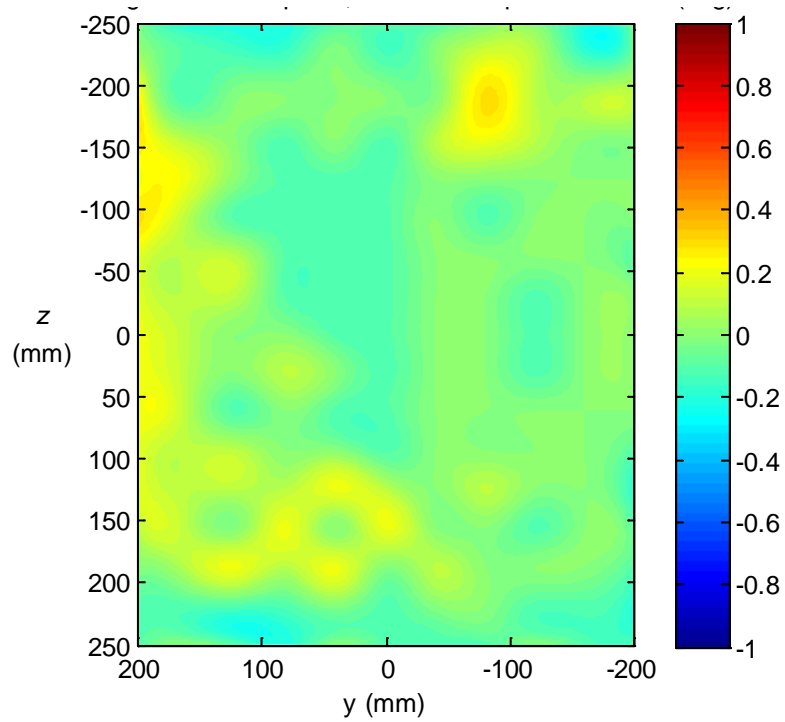
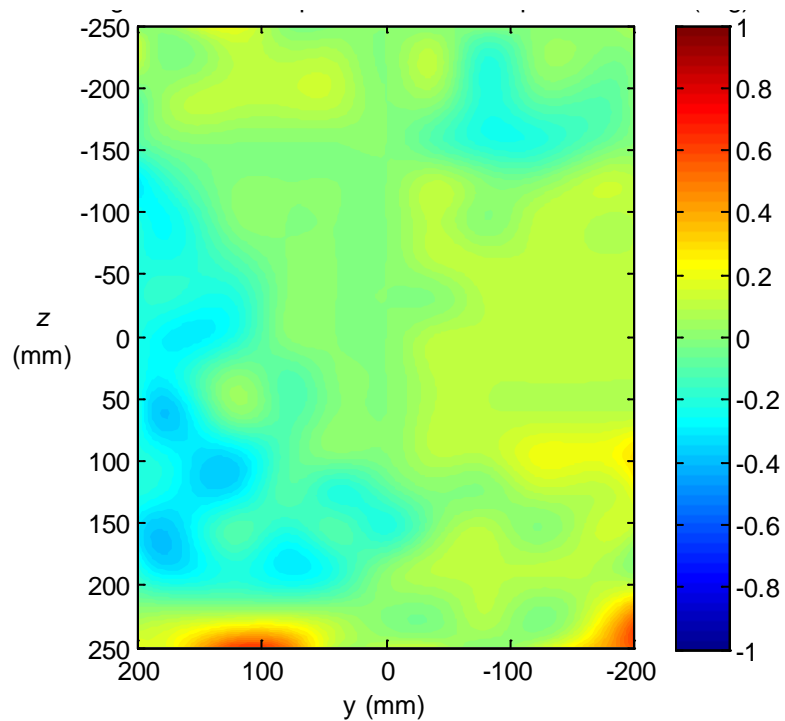


Figure 10 Contours of vertical and horizontal flow angles,  $\bar{U}_{\text{NOM}} = 10 \text{ m s}^{-1}$ , screens in tunnel.



(a) Vertical flow angles (degrees).



(b) Horizontal flow angles (degrees).

Figure 11 Contours of vertical and horizontal flow angles,  $\bar{U}_{\text{NOM}} = 20 \text{ m s}^{-1}$ , screens in tunnel.

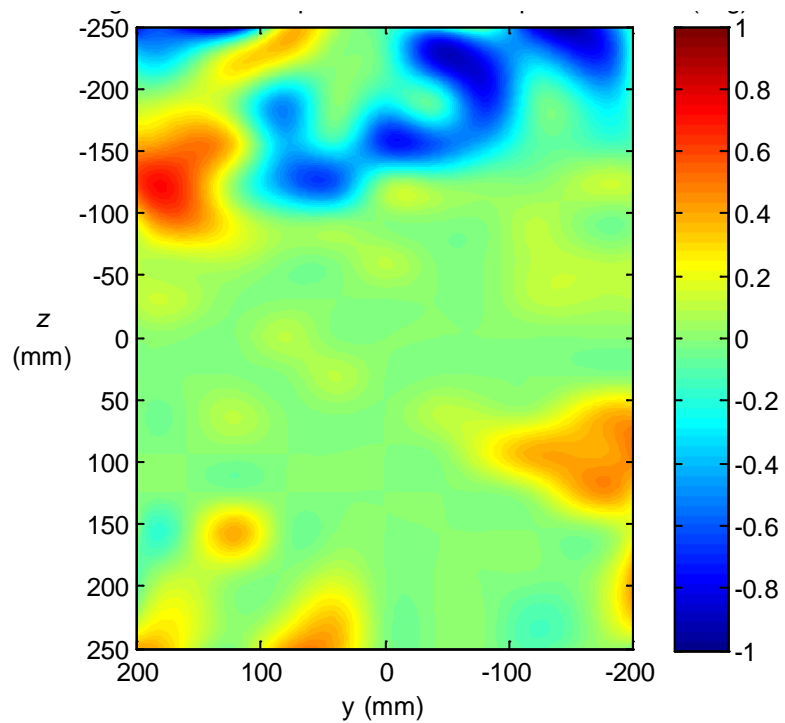
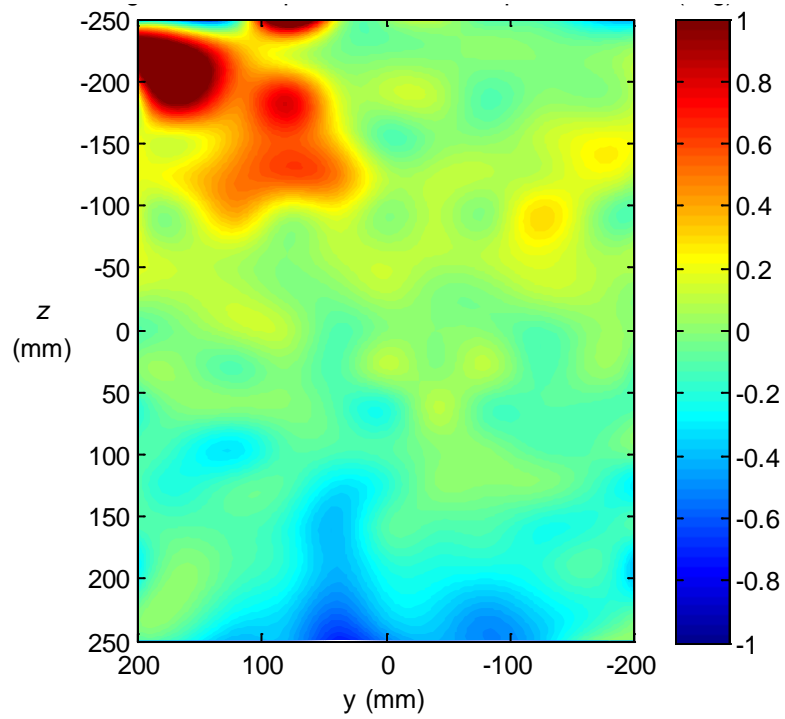


Figure 12 Contours of vertical and horizontal flow angles,  $\bar{U}_{\text{NOM}} = 10 \text{ m s}^{-1}$ , screens not in tunnel.

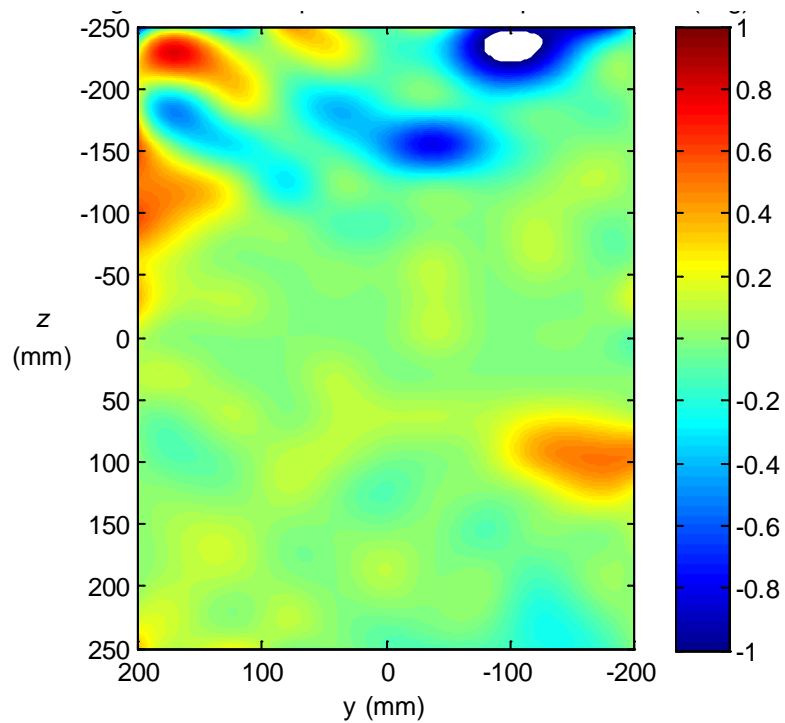
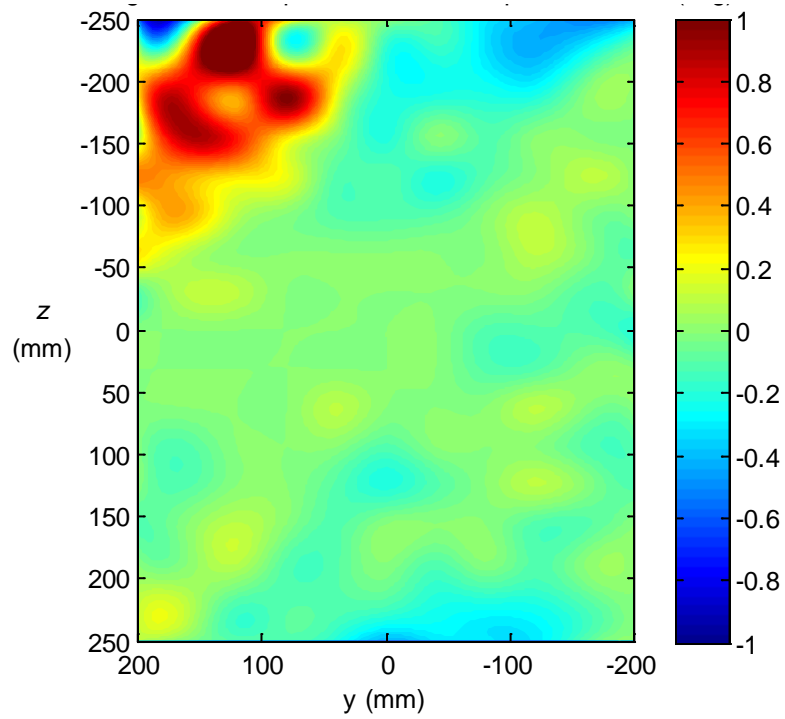


Figure 13 Contours of vertical and horizontal flow angles,  $\bar{U}_{\text{NOM}} = 20 \text{ m s}^{-1}$ , screens not in tunnel.

### 3.5 Uncertainty in Measured Flow Angles

When using the seven-hole probe, small uncertainties exist in measured flow angles due to probe setup errors and errors in instrumentation.

Probe setup errors occur since it is difficult to align precisely the seven-hole probe with the coordinate system of the RWT when measuring flow angles. The pitch angle of the seven-hole probe was set by carefully measuring distances from the probe body to the floor of the test section at two locations along the probe. Similarly, the yaw angle was set by measuring two distances from the probe body to a side wall of the test section. Using this method, the probe setup errors were about  $\pm 0.05^\circ$  for both pitch and yaw angles.

Considering instrumentation errors, it is important to note that the seven-hole probe was used for measurements at a velocity different from that at which the probe was calibrated. The probe had not been calibrated below Mach 0.2, corresponding to a velocity of about  $68 \text{ m}\cdot\text{s}^{-1}$ . The calibration was provided by Aeroprobe Corporation. In the current investigation, the probe was used for measurements at 10 and  $20 \text{ m}\cdot\text{s}^{-1}$ . The probe is quoted to measure flow angles to an accuracy of less than  $0.4^\circ$  and total flow velocities to an accuracy of less than  $0.8\%$ <sup>4</sup>. Since the probe was used at off-design flow conditions, uncertainties in measured flow angles and velocities may be greater than these quoted values.

## 4. Turbulence-Intensity Measurements

### 4.1 Test Schedule

Longitudinal or  $u$ -component turbulence intensities were measured in the test section of the tunnel at the 187 grid locations shown in Figure 2 at  $x_T = 0.0 \text{ mm}$  for  $\bar{U}_{\text{NOM}} = 10$  and  $20 \text{ m}\cdot\text{s}^{-1}$ . Measurements were taken both with and without screens in the tunnel.

### 4.2 Procedure Used to Measure Turbulence Intensities

Longitudinal turbulence intensities at the different grid locations in the test section of the RWT were measured using a constant-temperature hot-wire anemometer, manufactured at DST Group according to the design of Watmuff (1994), in conjunction with a DANTEC 55P01 single-wire probe having its original tungsten filament. (Tungsten filaments on DANTEC probes are often replaced with Wollaston-wire filaments). The hot-wire anemometer was interfaced with a Microstar data-acquisition unit, which in turn was interfaced with the computer, enabling fluctuating hot-wire output voltages to be sampled. Details of how to use the anemometer are given by Erm (2015). The probe was attached to the overhead traversing mechanism, with the filament oriented horizontally on the probe. The tip of the probe was manually positioned at the measurement grid, i.e. at  $x_T = 0 \text{ mm}$ , at each  $y_T$  location in turn, and was moved vertically in the  $z_T$  direction using

---

<sup>4</sup> See Product Manual V. 3.0 May 2012, Conventional 5 and 7 hole probes, published by Aeroprobe Corporation.

the traversing mechanism. The hot wire was calibrated in the conventional manner. During calibration, and when measuring turbulence intensities, hot-wire output voltages were sampled 15000 times at a sampling frequency of 1000 Hz. These sampling parameters resulted in convergence of calculated data. Further details on the measurement of turbulence intensities are given by Erm (2015).

### 4.3 Analysis of Turbulence Intensities

Contours of  $u$ -component turbulence intensities,  $\sqrt{\overline{u^2}}/\bar{U}$  %, for  $\bar{U}_{\text{NOM}} = 10$  and  $20 \text{ m}\cdot\text{s}^{-1}$ , when the screens were in the tunnel, are given in Figure 14. Corresponding plots when the screens were not in the tunnel are given in Figure 15.

An analysis of Figure 14 shows that the turbulence intensity is less than 0.4% across the grid, for  $\bar{U}_{\text{NOM}} = 10$  and  $20 \text{ m}\cdot\text{s}^{-1}$ . Similarly, an analysis of Figure 15 shows that the turbulence intensity is greater than 1% across the grid, for  $\bar{U}_{\text{NOM}} = 10$  and  $20 \text{ m}\cdot\text{s}^{-1}$ . The variations in turbulence intensities are more pronounced near the edges of the grid, particularly at the top of the grid. The higher turbulence intensities when the screens were not in the tunnel is to be expected.

### 4.4 Uncertainty in Measured Turbulence Intensities

There are small uncertainties in measured turbulence intensities,  $\sqrt{\overline{u^2}}/\bar{U}$ , due to small errors in instrumentation readings and also the fact that a calibration of a single hot wire may have drifted slightly between the start and finish of a set of measurements. However, any errors in measured velocities due to drifting of the calibration would largely be cancelled out due to the fact that intensities are determined as a quotient of velocities. Uncertainties in measured turbulence intensities are about  $\pm 0.01$  percentage points. For example, if the measured value of  $\sqrt{\overline{u^2}}/\bar{U}$  was 0.3%, then its value could range from 0.29% to 0.31%.

## 5. Assessment of Flow Quality in the RWT

It has been shown that the flow in the test section of the RWT has some non-uniformity in terms of mean-velocity deviations, flow angularity and turbulence intensities. The most important area of the test section, where models are usually located, is the region comprising approximately the central 0.7 of the width and 0.7 of the height, i.e. approximately the central 50% of the cross-sectional area of the test section. In the following, flow non-uniformities are quoted for the central region of the test section.

### 5.1 Mean Velocities

For the case when the screens were in the tunnel, for  $\bar{U}_{\text{NOM}} = 10$  and  $20 \text{ m}\cdot\text{s}^{-1}$ , the range of variation of velocity deviations,  $(\bar{U} - \bar{U}_0)/\bar{U}_0$ , was about 0.5%. When the screens were not in the tunnel, the range of variation of  $(\bar{U} - \bar{U}_0)/\bar{U}_0$  was about 1.4% for these two velocities.

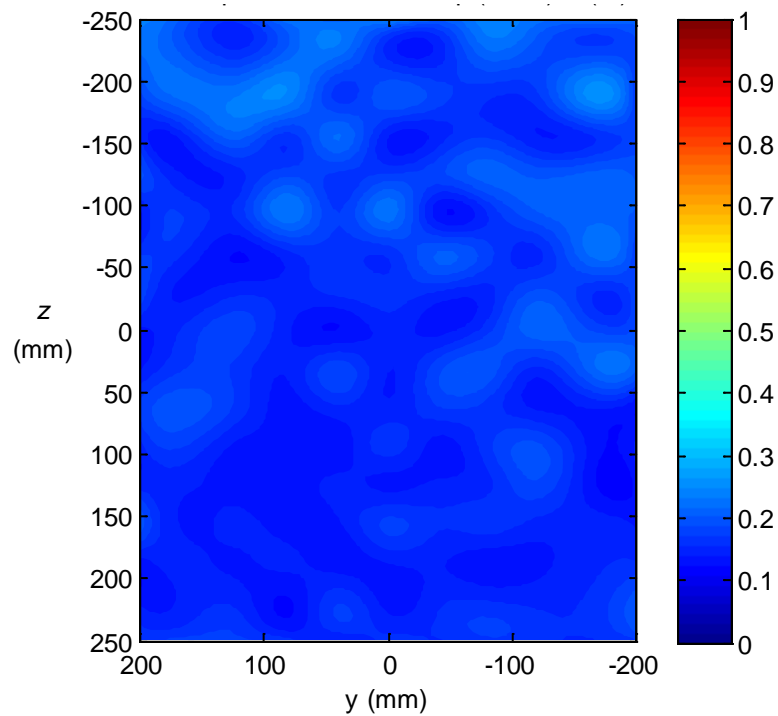
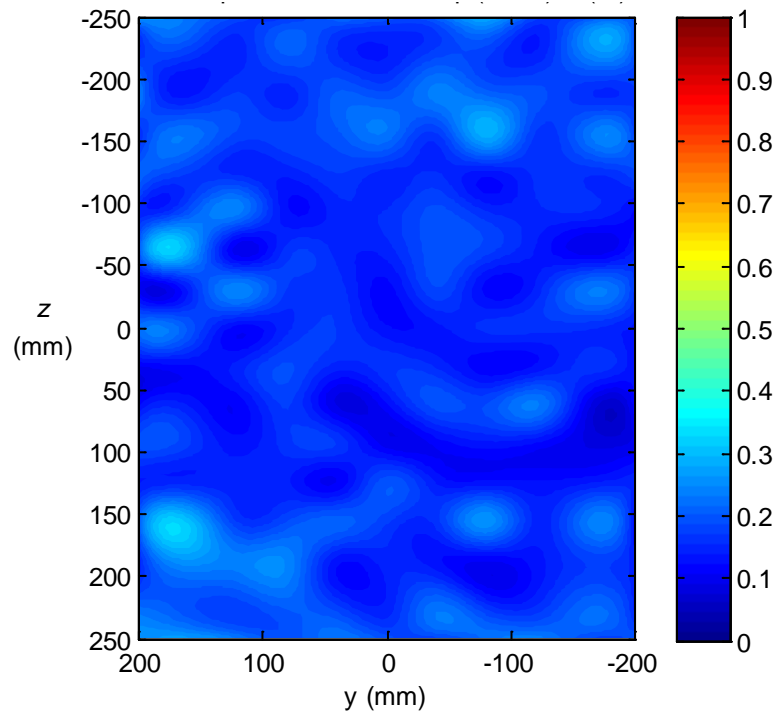


Figure 14 Contours of  $u$ -component intensities,  $\sqrt{\overline{u^2}}/\bar{U}$  %,  $\bar{U}_{\text{NOM}} = 10$  and  $20 \text{ m}\cdot\text{s}^{-1}$ , screens in tunnel.

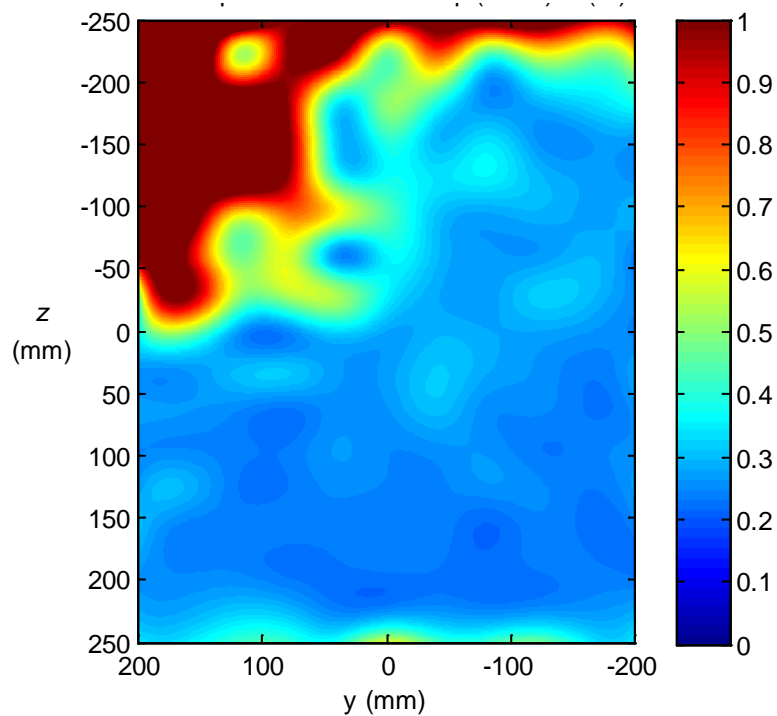
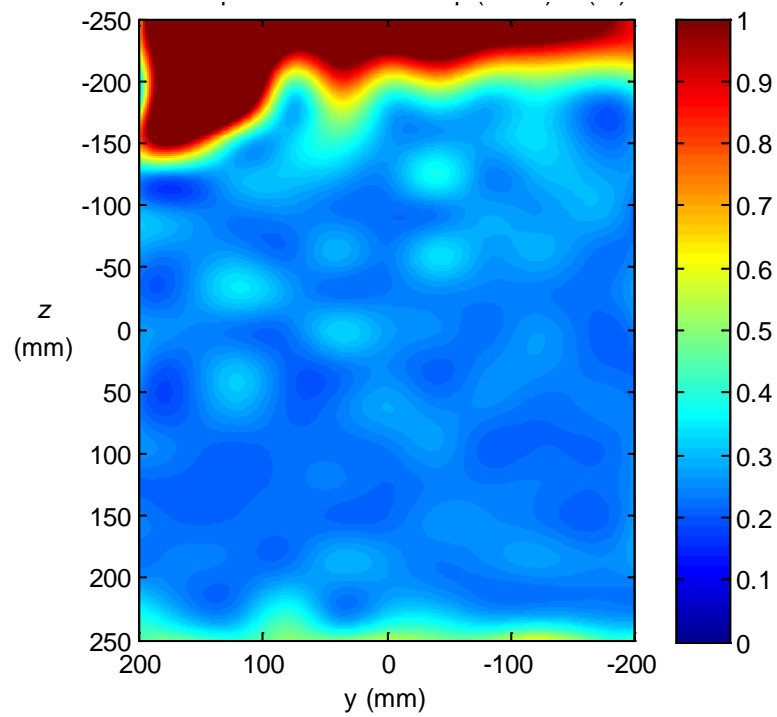


Figure 15 Contours of  $u$ -component intensities,  $\sqrt{\overline{u^2}}/\bar{U}$  %,  $\bar{U}_{\text{NOM}} = 10$  and  $20 \text{ m}\cdot\text{s}^{-1}$ , screens not in tunnel.

Rae & Pope (1984) indicate that acceptable longitudinal mean-velocity deviations across the test section are often quoted in the range  $\pm 0.20\%$  to  $\pm 0.30\%$  variation from the average value of the mean velocity. Bradshaw & Pankhurst (1964) indicate that acceptable mean-velocity variations across the test section of a high performance tunnel are less than  $\pm 0.2\%$ . According to Gorlin & Slezinger (1966), velocities should not deviate from the mean value by more than  $\pm 0.75\%$ .

## 5.2 Flow Angles

For the case when the screens were in the tunnel, for  $\bar{U}_{\text{NOM}} = 10$  and  $20 \text{ m}\cdot\text{s}^{-1}$ , the range of variation of horizontal and vertical flow angles was about  $0.5^\circ$ . When the screens were not in the tunnel, the range of variation of flow angles was about  $1.0^\circ$  for these two velocities.

According to Rae & Pope (1984), it would be desirable to have horizontal and vertical flow angle variations of less than  $\pm 0.10^\circ$ , but if this cannot be achieved, then the variations should be held to within  $\pm 0.20^\circ$ . Bradshaw & Pankhurst (1964) indicate that acceptable flow angle variations for a high performance tunnel are  $\pm 0.1^\circ$ . According to Gorlin & Slezinger (1966), horizontal and vertical flow angles should not deviate from the axial direction by more than  $\pm 0.25^\circ$ .

## 5.3 Turbulence Intensities

When the screens were in the tunnel, for  $\bar{U}_{\text{NOM}} = 10$  and  $20 \text{ m}\cdot\text{s}^{-1}$ , turbulence intensities,  $\sqrt{\overline{u^2}}/\bar{U}$ , were below  $0.3\%$ . When the screens were not in the tunnel, turbulence intensities were below  $0.5\%$  for  $\bar{U}_{\text{NOM}} = 10 \text{ m}\cdot\text{s}^{-1}$  and slightly greater than  $1\%$  for  $\bar{U}_{\text{NOM}} = 20 \text{ m}\cdot\text{s}^{-1}$ .

Bradshaw (1964) indicates that a root-mean-square  $u$ -component fluctuation of  $0.1\%$  of the mean velocity is often quoted as low enough for most experiments and that the best low-turbulence research tunnels have a turbulence intensity of the order of  $0.02\%$  at low speeds. Rae & Pope (1984), indicate that tunnels used for developmental testing can have longitudinal turbulence intensities as high as  $0.5\%$ .

## 5.4 Adequacy of Flow Quality in the RWT

The variations in mean velocities, flow angles and turbulence intensities across the test section of the RWT, for the case when the screens are in the tunnel, are within the acceptable ranges quoted in the literature. Excessive variations in flow conditions occur when the screens are not in the tunnel, so it is inadvisable to use the tunnel without screens.

The question of whether the quality of the flow in the tunnel is adequate for a given type of test depends upon the test to be undertaken. For flow-visualization investigations, where qualitative rather than quantitative answers are often required, the quality of the flow is adequate. The variations in mean velocities and flow angles across the flow are not excessive from the viewpoint of being able to measure meaningful forces and moments on models, provided care is taken manufacturing models so that they are geometrically similar to full-size vehicles. Small models cannot be manufactured to the same geometric

fidelity as larger models. For experiments studying boundary-layer transition, free-stream turbulence intensities should be low since high intensities can cause unwanted early transition. Longitudinal turbulence intensities of 0.1% to 0.5%, similar to the range in the RWT when the screens are in the tunnel, are classed as moderate turbulence levels by Coles (1962), so that the tunnel may not be suitable for studying transition phenomena.

## 6. Possible Ways of Improving the Flow in the RWT

Flow irregularities in the test sections of wind tunnels may arise from a number of different flow mechanisms and generally it is not possible to identify with certainty the causes of these irregularities simply by analysing measured calibration data. For the RWT, which has an open return circuit, variations in mean velocities can be caused by flow separations in the contraction. Angularity in the flow can occur if the honeycomb has cells of an inappropriate size and aspect ratio (see below). Turbulence can be generated in the boundary layers on the tunnel walls and from the honeycombs and screens. Despite the uncertainties involved in making a precise assessment of the causes of flow irregularities in the test section of the RWT, it is possible to identify some of the likely causes and to suggest possible ways of improving the flow.

If the contraction in a wind tunnel is not well designed then an adverse pressure gradient can exist near its inlet, which can lead to either continuous or intermittent flow separation, depending on the magnitude of the adverse pressure gradient (Rae & Pope, 1984). Such separations can have a detrimental effect on the quality of the flow in the test section. The existing contraction in the RWT is geometrically similar to the original contraction in the LSWT (see Erm, 2000). The circuit of the LSWT was modified by extending the length of the test section and installing a redesigned contraction (see Erm, 2003). This was done to enable longer models to be tested in the tunnel and also to possibly obtain some improvement of the quality of the flow. The installation of the extended test section and new contraction in the LSWT was found to only have a minimal effect on improving the quality of the flow. Perhaps the RWT could be modified in a similar manner.

Screens and honeycombs are known to improve the quality of the flow in test sections of tunnels, both in terms of improved longitudinal and lateral mean-velocity distributions and reduced longitudinal and lateral turbulence intensities. Screens reduce longitudinal components of mean velocities and intensities more than lateral components, as for a contraction, whereas honeycombs reduce lateral components of mean velocities and intensities more than longitudinal components.

The RWT has recently been fitted with three new screens so that it is not necessary to modify the screens to improve the flow. The honeycomb in the RWT has square cells whose frontal dimensions are 45 mm by 45 mm and the depth of the cells is 190 mm (approximate dimensions). The diameter of a circle having the same cross-sectional area of a square cell is about 50.8 mm, so that the ratio of the depth of the cells to the effective diameter of the cells is about 3.7:1, which is significantly lower than the recommended aspect ratio of about 6:1 to 8:1 (Rae & Pope, 1984). The sizes of the cells in the honeycomb in the RWT are also larger than recommended. Scheiman & Brooks (1981) studied

honeycombs in wind tunnels and found that the honeycombs had cell sizes ranging from 1.6 mm to 9.5 mm and aspect ratios varying between 6:1 and 8:1. If it is decided that a new honeycomb is needed to improve the quality of the flow in the test section, then it should have cells with a smaller frontal area and a larger aspect ratio, and follow the design guidelines given above. It would be preferable to use a honeycomb having hexagonal cells since the pressure loss for this type of honeycomb is less than for honeycombs having square or circular cross sections (Rae & Pope, 1984).

Most likely there is not a single cause of the flow non uniformities in the RWT and it may be necessary to change more than one component of the tunnel to obtain a significant improvement in the quality of the flow in the test section. If any modifications are made to the RWT, it would be preferable that they be carried out in stages to access the effects of each modification.

## 7. Concluding Remarks

A detailed calibration of the flow in the test section of the Research Wind Tunnel at DST Group is given in this report. Longitudinal mean velocities, horizontal and vertical flow angles, and  $u$ -component (longitudinal) turbulence intensities were measured for nominal free-stream velocities of 10 and 20 m·s<sup>-1</sup>. Measurements were taken at 187 grid locations across the flow, at a single longitudinal position located half way along the test section, both with and without screens in the tunnel.

Longitudinal mean-flow velocities were measured using a Pitot-static probe, flow angles were measured using a seven-hole pressure probe, and longitudinal turbulence intensities were measured using a single hot-wire probe attached to a constant-temperature hot-wire anemometer. The probes were mounted, in turn, on an overhead traversing mechanism, used to move the probes in the vertical direction. The probes could be positioned to an accuracy of  $\pm 0.5$  mm in the longitudinal direction (manual positioning),  $\pm 0.5$  mm in the transverse horizontal direction (manual positioning), and  $\pm 0.1$  mm in the transverse vertical direction (positioning using the traversing mechanism).

Considering approximately the central 50% of the cross-sectional area of the test section, the following flow non-uniformities were observed when the screens were in the tunnel. For  $\bar{U}_{\text{NOM}} = 10$  and 20 m·s<sup>-1</sup>, the range of variation of velocity deviations,  $(\bar{U} - \bar{U}_0)/\bar{U}_0$ , was about 0.5%, the range of variation of horizontal and vertical flow angles was about 0.5°, and turbulence intensities,  $\sqrt{\overline{u^2}}/\bar{U}$ , were below about 0.3%.

When the screens were in the tunnel, variations in mean velocities, flow angles and turbulence intensities across the flow are comparable with acceptable variations quoted in the literature. The tunnel is considered suitable for flow-visualization studies around models and the measurement of forces, moments and pressures on models. The tunnel may not be suitable for boundary-layer-transition studies, due to the moderate levels of free-stream turbulence levels in the tunnel. It is inadvisable to carry out tests in the tunnel when the screens are not installed.

It may be possible to improve the quality of the flow in the test section of the Research Wind Tunnel by modifying the shape of the contraction, as was done for the Low Speed Wind Tunnel, and also by installing a new honeycomb.

## **8. Acknowledgements**

The authors are grateful to Malcolm Jones for developing some software for the operation of the overhead traversing mechanism and to Chris Jones, from QinetiQ Engineering Services, for drawing some of the figures used in this report.

## 9. References

- Bradshaw, P. 1964 *Experimental Fluid Mechanics*, Pergamon Press Ltd, London, UK.
- Bradshaw, P. & Pankhurst, R. C. 1964 The design of low speed wind tunnels. *Progress in Aeronautical Sciences*, Vol. 5, Edited by D. Kucheman & L. H. G. Sterne, Pergamon Press, New York, USA.
- Chue, S. H. 1975 Pressure probes for fluid measurement. *Progress in Aerospace Sciences*, Vol. 16, No. 2, 1975.
- Coles, D. E. 1962 The turbulent boundary layer in a compressible fluid. *Rand Report R-403-PR*, Appendix A: A manual of experimental boundary layer practice for low-speed flow, September.
- Erm, L. P. 2000 Calibration of the flow in the test section of the low-speed wind tunnel at AMRL. DSTO-TR-1073. Defence Science and Technology Organisation, Melbourne, Australia.
- Erm, L. P. 2003 Calibration of the flow in the extended test section of the low-speed wind tunnel at DSTO. DSTO-TR-1384. Defence Science and Technology Organisation, Melbourne, Australia.
- Erm, L. P. 2015 Acquisition of turbulence data using the DST Group constant-temperature hot-wire anemometer system. DST-Group-TN-1467, Defence Science and Technology Group, Melbourne, Australia.
- Gorlin, S. M. & Slezinger, I. I. 1966 *Wind tunnels and their instrumentation*. Translated from Russian, Israel Program for Scientific Translations, Jerusalem.
- Rae, W. H. Jr. & Pope, A. 1984 *Low-speed wind tunnel testing*. John Wiley & Sons, New York, USA.
- Scheiman, J. & Brooks, J. D. 1981 Comparison of experimental and theoretical turbulence reduction from screens, honeycomb, and honeycomb-screen combinations. *JAS*, Vol. 18, pp. 638-643, 1981.
- Watmuff, J. H. 1994 A high-performance constant-temperature hot-wire anemometer. NASA Contractor Report 177645.

<b>DEFENCE SCIENCE AND TECHNOLOGY GROUP DOCUMENT CONTROL DATA</b>				1. DLM/CAVEAT (OF DOCUMENT)	
2. TITLE  Calibration of the Flow in the Test Section of the Research Wind Tunnel at DST Group		3. SECURITY CLASSIFICATION (FOR UNCLASSIFIED REPORTS THAT ARE LIMITED RELEASE USE (L) NEXT TO DOCUMENT CLASSIFICATION)  Document (U) Title (U) Abstract (U)			
4. AUTHOR(S)  Lincoln P. Erm and Paul P. E. Jacquemin		5. CORPORATE AUTHOR  Defence Science and Technology Group 506 Lorimer St Fishermans Bend Victoria 3207 Australia			
6a. DST Group NUMBER DST Group-TN-1468	6b. AR NUMBER AR-016-436	6c. TYPE OF REPORT Technical Note	7. DOCUMENT DATE October 2015		
8. FILE NUMBER eg: 2014/1179364/1	9. TASK NUMBER ERP07/299	10. TASK SPONSOR CDS	11. NO. OF PAGES 24	12. NO. OF REFERENCES 11	
13. DST Group Publications Repository  <a href="http://dspace.dstg.defence.gov.au/dspace/">http://dspace.dstg.defence.gov.au/dspace/</a>		14. RELEASE AUTHORITY  Chief, Aerospace Division			
15. SECONDARY RELEASE STATEMENT OF THIS DOCUMENT  <i>Approved for public release</i>  <small>OVERSEAS ENQUIRIES OUTSIDE STATED LIMITATIONS SHOULD BE REFERRED THROUGH DOCUMENT EXCHANGE, PO BOX 1500, EDINBURGH, SA 5111</small>					
16. DELIBERATE ANNOUNCEMENT  No Limitations					
17. CITATION IN OTHER DOCUMENTS		Yes			
18. DSTG RESEARCH LIBRARY THESAURUS  Low speed wind tunnels, Calibration, Measurement, Velocity, Flow, Turbulence					
19. ABSTRACT Results are given of a detailed calibration of the flow in the test section of the Research Wind Tunnel at DST Group. The calibration was performed to establish the flow quality and to provide guidance when determining the suitability of the tunnel for given tests. Longitudinal mean-flow velocities, flow angles and longitudinal-component turbulence intensities were measured at up to 187 grid locations across the flow at the centre of the test section for nominal free-stream velocities of 10 and 20 m·s <sup>-1</sup> . Measurements were taken when screens were installed in the tunnel and when there were no screens in the tunnel. The most important area of the test section, where models are usually located, is the region comprising approximately the central 50% of the cross-sectional area of the test section. In this region, the following flow non-uniformities were observed when screens were in the tunnel. For nominal free-stream velocities of 10 and 20 m·s <sup>-1</sup> , velocity deviations varied by about 0.5%, horizontal and vertical flow angles varied by about 0.6°, and longitudinal-component turbulence intensities were below about 0.3%. The variations in flow parameters are comparable with acceptable variations quoted in the literature. Based on these measurements, the tunnel is considered suitable for flow-visualization studies around models and the measurement of forces, moments and pressures on models. The tunnel may not be suitable for boundary-layer-transition studies, due to the moderate levels of free-stream turbulence levels in the tunnel. Possible ways of modifying the tunnel to improve the flow in the test section are suggested.					